Vol 18 No 12, December 2009
1674-1056/2009/18(12)/5443-08

Chinese Physics B

© 2009 Chin. Phys. Soc.
and IOP Publishing Ltd

Kondo effect in a deformed molecule coupled asymmetrically to ferromagnetic electrodes*

Wang Rui-Qiang(王瑞强)[a)†] and Jiang Kai-Ming(蒋开明)[b)]

[a)] *Laboratory of Quantum Information Technology, Institute for Condensed Matter Physics, and School of Physics and Telecommunication Engineering, South China Normal University, Guangzhou* 510006, *China*

[b)] *Department of Physics, Shanghai Maritime University, Shanghai* 201306, *China*

(Received 21 July 2009; revised manuscript received 15 September 2009)

The nonequilibrium Kondo effect is studied in a molecule quantum dot coupled asymmetrically to two ferromagnetic electrodes by employing the nonequilibrium Green function technique. The current-induced deformation of the molecule is taken into account, modeled as interactions with a phonon system, and phonon-assisted Kondo satellites arise on both sides of the usual main Kondo peak. In the antiparallel electrode configuration, the Kondo satellites can be split only for the asymmetric dot-lead couplings, distinguished from the parallel configuration where splitting also exists, even though it is for symmetric case. We also analyze how to compensate the splitting and restore the suppressed zero-bias Kondo resonance. It is shown that one can change the TMR ratio significantly from a negative dip to a positive peak only by slightly modulating a local external magnetic field, whose value is greatly dependent on the electron–phonon coupling strength.

Keywords: Kondo effect, molecular spintronics, tunneling magnetoresistance, electron–phonon interaction, nonequilibrium Green function

PACC: 7225, 6320K

1. Introduction

When a quantum dot (QD) with local odd-spins is coupled to two external electrodes, at low enough temperatures, the local spin can be screened by the spin of a conduction electron coming from the electrodes, resulting in the so-called Kondo effect (anomaly). The Kondo anomaly is generally detected by measuring the resonant conductance peak at zero-bias voltage or the sharp peak of density of states (DOS) at the Fermi energy level. While the normal Kondo effect,[1,2] associated with electronic transports through a QD attached to normal metal electrodes, is well-understood both in theory and in experiment, there has been great interest in understanding the ferromagnetic Kondo effect,[3,4] where the QD is coupled to ferromagnetic metal electrodes.[5]

Several years ago, different theoretical methods were devoted to this field. Studies of some methods, involving scaling arguments,[3] the equation of motion,[6] the noncrossing approximation,[7] and the numerical renormalization group,[8] suggested that the zero-bias Kondo peak should be split for the parallel (P) alignment in magnetic moments of two ferromagnetic electrodes. However, the slave-boson mean-field method and other theories[9,10] predicted opposite results. Recently, the dispute has been mediated, and the splitting of the zero-bias Kondo peak was first observed experimentally by Abhay *et al*[11] in a C_{60}-molecular QD tunnel junction. Then, an experiment was repeated in a similar setup with a semiconductor QD[12] instead, where not only the splitting of the Kondo resonant peak but also its restoration is demonstrated by applying an external magnetic field. An external field with $B = 1.2$ T can completely compensate the effective exchange field induced by the leads' magnetism and makes the splitting of the Kondo peak disappear. As a further exploration, Hauptmann *et al*[13] replaced the semiconductor QD with a carbon nanotube QD and observed additionally that the effective exchange field itself and hence the local spin polarization can be tuned and reversed merely by tuning the gate voltage. It is theoretically revealed that the underlying mechanism of the Kondo peak splitting is attributed to charge fluctuations. Owing to mismatch in the DOS for the spin majority and spin minority, the charge fluctuations associated with the

*Project supported by the National Natural Science Foundation of China (Grant No 10974058), the Shanghai Natural Science Foundation of China (Grant No 09ZR1421400), Science and Technology Program of Shanghai Maritime University (Grant No 2008475), and Postdoctoral Science Foundation of Jiangsu Province of China (Grant No 0802008C).

†Corresponding author. E-mail: rqwanggz@163.com

electron tunneling into and out of the dot will renormalize the bare energy level in the dot. As a consequence, the spin-degenerated energy level is lifted, equivalent to the contribution from an effective exchange field.[3,14,15]

On the one hand, with further shrinking in the size of spintronic devices, molecular spintronics[16] or nanospintronics[17] have emerged rapidly as a new branch of spintronics. Compared to conventional electronic devices based on semiconductor QDs, such molecular-scale electronic devices have a very small size and manifest themselves with pronounced discrete dot levels as well as large charging energies. Therefore, the molecular tunnel junction provides a powerful tool to observe the Kondo anomaly.[11,18,19] As opposed to "hard" semiconductor QDs, molecular QDs are "soft". If a tunneling electron travels through a molecular QD, the molecule will deform from a sphere to a prolate ellipsoid, giving rise to the quantum excitation of internal vibrational (phonon) modes.[20,21] For instance, in nonmagnetic single-molecule transistors,[1,20,22] the electron tunneling spectrum shows inelastic vibrational sidebands even in the Kondo regime. For the same reason, it is expected that electron–phonon interaction (EPI) can modulate the transport of spin-polarized electrons in a molecular QD connected with ferromagnetic electrodes. Due to the participation of the phonon modes, there appear lots of interesting phenomena in spintronics, such as the oscillation of tunneling magnetoresistance (TMR) with applied bias voltage,[23,24] the vibration-mediated Kondo effect,[25,26] and the spin valve effect.[27]

In a recent paper,[25] we have studied the EPI influence on the Kondo effect in a single-molecular QD symmetrically coupled to ferromagnetic electrodes, where the vibration-mediated spin splitting of Kondo satellites occurs for the P magnetic alignment but not for the antiparallel (AP) one. In the present paper, we will focus on another two aspects: 1) the vibration-mediated Kondo satellites can be also split for AP alignment when there exist asymmetric couplings between dot and leads. Moreover, the split Kondo subpeaks in differential conductance for the P and AP alignments show different tilted profiles with respect to the bias voltage, and thus the TMR ratio exhibits a considerable asymmetry with respect to the bias voltage; 2) the suppressed zero-bias Kondo resonance due to spin splitting can be restored by applying an external magnetic field, whose magnitude is significantly dependent on the EPI strength. This paper is organized as follows. In Section 2 the theoretical model is presented. In Section 3 the influence of the coupling asymmetry and the external magnetic field on the Kondo anomaly is discussed. Finally, a brief summary is given in the last section.

2. Model and method

The Hamiltonian for an electron–electron interacting molecular QD, coupled to two ferromagnetic electrodes and to a phonon bath, can be written as a typical Anderson–Holstein model:

$$H = H_{\rm L} + H_{\rm R} + H_{\rm ph} + H_{\rm D} + H_{\rm T}. \tag{1}$$

The first two terms describe the non-interacting electron reservoirs $H_\alpha = \sum_{k\sigma} \varepsilon_{k\sigma,\alpha} c^\dagger_{k\sigma,\alpha} c_{k\sigma,\alpha}$ (α=L, R), where $c^\dagger_{k\sigma,\alpha}(c_{k\sigma,\alpha})$ is the creation (annihilation) operator for an electron with energy $\varepsilon_{k\sigma,\alpha}$, wave vector k, and spin σ. Free phonon mode $H_{\rm ph} = \hbar\omega_0 a^\dagger a$, with the vibration frequency ω_0 and the creation (annihilation) operator $a^\dagger$ (a) for a phonon, is applied to simulate the molecular deformation. The molecule is assumed as a single energy-level QD, $H_{\rm D} = \sum_\sigma [\varepsilon_\sigma + eV_{\rm g} + \lambda(a^\dagger + a)] d^\dagger_\sigma d_\sigma + U d^\dagger_\uparrow d_\uparrow d^\dagger_\downarrow d_\downarrow$, where $d^\dagger_\sigma$ (d_σ) creates (annihilates) a dot electron with spin σ, λ is the EPI coupling strength, and U is the on-site Coulomb repulsion between electrons. The energy level ε_σ of the QD is controlled by a gate voltage $V_{\rm g}$. When an external magnetic field B is exerted on the spin of the dot electron, the Zeeman energy enters the energy level in the form $\varepsilon_{\uparrow(\downarrow)} = \varepsilon_0 \pm g u_{\rm B} B$. The last term in Eq.(1) is the tunneling Hamiltonian, given by $H_{\rm T} = \sum_{k\sigma,\alpha} T_{k\sigma,\alpha} c^\dagger_{k\sigma,\alpha} d_\sigma + {\rm H.c.}$ Due to the electron tunneling between the dot and leads, the dot energy level is broadened by the bandwidth function, $\Gamma_{\alpha,\sigma} = 2\pi\rho_{\alpha,\sigma} \sum_k |T_{k\sigma,\alpha}|^2$, with $\rho_{\alpha,\sigma}$ denoting the DOS of σ-spin electrons in lead α at the Fermi level.

It is easy to derive the formula of the current through the system by using the Keldysh nonequilibrium Green function approach[28]

$$I_\sigma = \frac{-e^2}{\hbar} \int \frac{{\rm d}\omega}{2\pi} [f_{\rm L}(\omega) - f_{\rm R}(\omega)] \times \frac{\Gamma_{{\rm L},\sigma}\Gamma_{{\rm R},\sigma}}{\Gamma_{{\rm R},\sigma} + \Gamma_{{\rm L},\sigma}} {\rm Im}\, G^r_\sigma(\omega), \tag{2}$$

where $G^r_\sigma(\omega)$ is the retarded Green function for a σ-spin electron in the QD. $f_\alpha(\omega) = 1/\{1 + \exp[(\omega - \mu_\alpha)/k_{\rm B}T]\}$ is the Fermi–Dirac distribution function in lead α, with the electrochemical potentials $\mu_{\rm L} = -\mu_{\rm R} = eV_{\rm bias}/2$, where $V_{\rm bias}$ is an applied bias voltage.

In order to calculate the retarded Green function $G^r_\sigma(\omega)$we should eliminate the electron–phonon coupling part in $H_{\rm D}$ by using the canonical transformation with $s = \lambda/\hbar\omega_0 \sum_\sigma d^\dagger_\sigma d_\sigma(a^\dagger - a)$. After that, equation (1) is transformed into $\tilde{H} = e^s H e^{-s} = \tilde{H}_{\rm el} + H_{\rm ph}$, where

$$\begin{aligned}\tilde{H}_{\rm el} = &\sum_\sigma(\tilde{\varepsilon}_\sigma + eV_{\rm g})d^\dagger_\sigma d_\sigma + \tilde{U}d^\dagger_\uparrow d_\uparrow d^\dagger_\downarrow d_\downarrow \\ &+ \sum_{k\sigma,\alpha}\varepsilon_{k\sigma,\alpha}c^\dagger_{k\sigma,\alpha}c_{k\sigma,\alpha} \\ &+ \sum_{k\sigma,\alpha}(\tilde{T}_{k\sigma,\alpha}c^\dagger_{k\sigma,\alpha}d_\sigma + {\rm H.c.}). \end{aligned} \tag{3}$$

Here, the resulting parameters are renormalized, i.e., $\tilde{\varepsilon}_\sigma = \varepsilon_\sigma - g\hbar\omega_0$, $\tilde{U} = U - 2g\hbar\omega_0$ with $g = (\lambda/\hbar\omega_0)^2$, and the tunneling matrix elements $\tilde{T}_{k\sigma,\alpha} = T_{k\sigma,\alpha}X$ with $X = \exp[-\lambda/\hbar\omega_0(a^\dagger - a)]$. Assuming the phonon bath remains in thermal equilibrium in the process of the electron tunneling, one may replace $\tilde{T}_{k\sigma,\alpha}$ approximately with its expectation value,[24,29,30] $\tilde{T}_{k\sigma,\alpha} = T_{k\sigma,\alpha}\langle X\rangle = T_{k\sigma,\alpha}{\rm e}^{-g(N_{\rm ph}+1/2)}$ with $N_{\rm ph} = 1/[\exp(\hbar\omega_0/k_{\rm B}T) - 1]$ as the averaged phonon number. Thus, the renormalized Hamiltonian for electrons $\tilde{H}_{\rm el}$ becomes a typical Anderson model, and the corresponding retarded Green function $\tilde{G}^r_\sigma(\omega)$ can be obtained with the help of the equation of motion (EOM) approach,[31]

$$\begin{aligned}\tilde{G}^r_\sigma(\omega) = &\frac{1 - \langle d^\dagger_{\bar\sigma}d_{\bar\sigma}\rangle}{\omega - \tilde{\varepsilon}_\sigma - eV_{\rm g} - \tilde{\Sigma}_{\sigma0} + \tilde{U}\Sigma_{\sigma1}(\omega - \tilde{\varepsilon}_\sigma - eV_{\rm g} - \tilde{U} - \tilde{\Sigma}_{\sigma0} - \tilde{\Sigma}_{\sigma3})^{-1}} \\ &+ \frac{\langle d^\dagger_{\bar\sigma}d_{\bar\sigma}\rangle}{\omega - \tilde{\varepsilon}_\sigma - eV_{\rm g} - \tilde{U} - \tilde{\Sigma}_{\sigma0} - \tilde{U}\tilde{\Sigma}_{\sigma2}(\omega - \tilde{\varepsilon}_\sigma - eV_{\rm g} - \tilde{\Sigma}_{\sigma0} - \tilde{\Sigma}_{\sigma3})^{-1}}. \end{aligned} \tag{4}$$

The average occupation number of electrons on the QD, $\langle d^\dagger_{\bar\sigma}d_{\bar\sigma}\rangle$ with spin $\bar\sigma$ opposite to σ, is evaluated with a self-consistent equation, $\langle n_\sigma\rangle = -\int {\rm d}\omega(1/\pi)\bar{f}_\sigma(\omega){\rm Im}\, G^r_\sigma(\omega)$ with $\bar{f}_\sigma(\omega) = [\Gamma_{{\rm L},\sigma}f_{\rm L}(\omega) + \Gamma_{{\rm R},\sigma}f_{\rm R}(\omega)]/(\Gamma_{{\rm L},\sigma} + \Gamma_{{\rm R},\sigma})$. The self-energies in Eq.(4) are $\tilde{\Sigma}^r_{0\sigma}(\omega) = \sum_\alpha\int {\rm d}\varepsilon(1/2\pi)(\tilde{\Gamma}_{\alpha,\sigma}/(\omega - \varepsilon))$, and

$$\tilde{\Sigma}^r_{i\sigma}(\omega) = \sum_{\alpha\in{\rm L,R}}\int\frac{{\rm d}\varepsilon}{2\pi}\tilde{\Gamma}_{\alpha,\bar\sigma}A_i(\varepsilon)\left(\frac{1}{\omega - \varepsilon - \tilde{\varepsilon}_\sigma + \tilde{\varepsilon}_{\bar\sigma}} + \frac{1}{\omega + \tilde{\varepsilon}_{k\bar\sigma} - \tilde{\varepsilon}_\sigma - \tilde{\varepsilon}_{\bar\sigma} - 2eV_{\rm g} - \tilde{U}}\right) \tag{5}$$

with $A_{i=1}(\varepsilon) = f_{\bar\sigma}(\varepsilon), A_{i=2}(\varepsilon) = 1 - f_{\bar\sigma}(\varepsilon), A_{i=3}(\varepsilon) = 1$, and $\tilde{\Gamma}_{\alpha,\sigma} = {\rm e}^{-g(2N_{\rm ph}+1)}\Gamma_{\alpha,\sigma}$. In the wide-band approximation, one can assume $\Gamma_{{\rm L}\sigma} = \Gamma_{\rm L0}(1 + \sigma_z P_{\rm L})$ and $\Gamma_{{\rm R}\sigma} = \Gamma_{\rm R0}(1 \pm \sigma_z P_{\rm R})$ with a constant $\Gamma_{\alpha0} = (\Gamma_{\alpha\uparrow} + \Gamma_{\alpha\downarrow})/2$ and sign $+(-)$ standing for the P (AP) magnetization alignment. The spin polarization of the ferromagnetic electrode α is described by $P_\alpha = (\rho_{\alpha,\uparrow} - \rho_{\alpha,\downarrow})/(\rho_{\alpha,\uparrow} + \rho_{\alpha,\downarrow})$.

The relation between the Fourier transformation of the Green function $G(t)$ associated with the original Hamiltonian in Eq.(1) and $\tilde{G}(t)$ associated with the dressed Hamiltonian in Eq.(3) can be found[24,25,29] to be

$$G^r_\sigma(\omega) = \sum_{n=-\infty}^{\infty} L_n\{[1 - \bar{f}_\sigma(\omega - n\hbar\omega_0)]\tilde{G}^r_\sigma(\omega - n\hbar\omega_0) + \bar{f}_\sigma(\omega + n\hbar\omega_0)\tilde{G}^r_\sigma(\omega + n\hbar\omega_0)\}, \tag{6}$$

where $L_n = {\rm e}^{-g(2N_{\rm ph}+1)}{\rm e}^{n\hbar\omega_0/2k_{\rm B}T}{\rm I}_n[2g\sqrt{N_{\rm ph}(N_{\rm ph}+1)}]$ with ${\rm I}_n(x)$ as the n-th Bessel function of the complex argument.

It is noted that in the Kondo regime both charge and spin fluctuations play an important role. The charge fluctuations will lead to renormalization for the bare energy level $\tilde{\varepsilon}_\sigma$ in the QD.[3,6,14,15,32] The renormalized procedure is introduced theoretically by employing a self-consistent calculation. For the case of normal metal as leads, the renormalized procedure will keep the energy level $\tilde{\varepsilon}_\sigma$ unchanged, but for ferromagnetic leads, it will give rise to spin splitting between two spin-degenerated energy levels, $\tilde{\varepsilon}_\uparrow$ and $\tilde{\varepsilon}_\downarrow$, due to the presence of magnetism. The self-consistent calculation follows from the renormalized group spirit and is confirmed to be comparable to the renormalization group scaling analysis,[3] not only accounting for the spin fluctuations but for the charge fluctuations. Here, the self-consistent calculation is extended to account for the inelastic scatter (polaronic effect). As a result, the energy $\tilde{\varepsilon}^{(\pm n)}_\sigma$ is renormalized to be $\breve{\varepsilon}^{(\pm n)}_\sigma$ with the shifted part being[3,6,14,15,32]

$$\begin{aligned}\delta\breve{\varepsilon}^{(\pm n)}_\sigma &= \breve{\varepsilon}^{(\pm n)}_\sigma - \tilde{\varepsilon}_\sigma = {\rm Re}[\tilde{\Sigma}^r_{0\sigma}(\breve{\varepsilon}_\sigma \pm n\hbar\omega_0) + \tilde{\Sigma}^r_{1\sigma}(\breve{\varepsilon}_\sigma \pm n\hbar\omega_0)] \\ &= -{\rm Re}\sum_{\alpha\in{\rm L,R}}\int\frac{{\rm d}\varepsilon}{2\pi}f_\alpha(\varepsilon)[\tilde{\Gamma}_{\alpha,\sigma}\left(\frac{1}{\varepsilon \pm n\hbar\omega_0 - \breve{\varepsilon}^{(\pm n)}_\sigma} + \frac{1}{-\varepsilon \pm n\hbar\omega_0 + \tilde{U} + \breve{\varepsilon}^{(\pm n)}_\sigma}\right), \end{aligned} \tag{7}$$

where the sign +(−) corresponds to the electron (hole) transport, accompanied by n-phonon emission. The spin splitting between $\breve{\varepsilon}_{\uparrow}^{(\pm n)}$ and $\breve{\varepsilon}_{\downarrow}^{(\pm n)}$ is equivalent to the role of an effective exchange field, $gu_{\rm B}B_{\rm eff}^{(\pm n)} = \sum_{\alpha\in{\rm L,R}}(\delta\breve{\varepsilon}_{\uparrow}^{(\pm n)} - \delta\breve{\varepsilon}_{\downarrow}^{(\pm n)})$.

3. Numerical results and discussions

In this section, based on the formulas outlined above, we will discuss numerical results. In order to describe the asymmetric coupling between the QD and two ferromagnetic leads for convenience, we define an asymmetry factor as $\eta = (\Gamma_{\rm L0} - \Gamma_{\rm R0})/\Gamma_0$ with $\Gamma_0 = \Gamma_{\rm L0} + \Gamma_{\rm R0}$. The factor η characterizes the difference between the left-dot and the right-dot tunnel barriers in an asymmetric double-barrier tunnel junction with the molecular QD. The asymmetry becomes prominent with η increasing; in the extreme case, $\eta = 0$, it corresponds to the symmetric situation, and $\eta = 1$ corresponds to the situation that the right-dot contact is insulated. We consider the ferromagnetic metal Ni as two electrodes, which is extensively adopted in experiments[11−13] and whose polarization is regarded as $P_{\rm L} = P_{\rm R} = 0.31$. Some other parameters are fixed for our numerical calculations: $U = 50$, $\Gamma_0 = 0.4$, $k_{\rm B}T = 10^{-4}$, $eV_{\rm g} = 0$, and $\tilde{\varepsilon}_\sigma = \tilde{\varepsilon}_{\bar{\sigma}} = \tilde{\varepsilon}_0 = -0.5$ in the absence of external magnetic field B. All the energies are measured relative to the phonon energy $\hbar\omega_0$.

We plot spin-resolved DOSs, $\rho_{\uparrow(\downarrow)} = -(1/\pi){\rm Im}\, G^r_{\uparrow(\downarrow)}(\omega)$, as functions of electron energy ω for the AP configuration in Fig.1, where the Kondo resonance and phonon-assisted Kondo satellites are clearly observable. For the symmetric coupling $\eta = 0$ (solid lines), the curves of the spin-up and spin-down overlap at the Fermi level and there is no spin splitting because the effective exchange fields arising from two leads cancel each other out for the AP magnetic configuration. The Kondo satellites are exactly located at energies $\omega = \pm n\hbar\omega_0$ with $n = 1, 2\ldots$. However, if the system is asymmetric, i.e. $\eta \neq 0$, spin splitting of the Kondo anomaly appears. The spin-up Kondo peak, together with its Kondo satellites, shifts to the lower energy regime, and the spin-down counterpart shifts to the opposite side. This shift is a consequence of an effective exchange field $B_{\rm eff}^{(\pm n)}$. The phonon emission of holes is responsible for the left Kondo satellites and the phonon emission of electrons for the right Kondo satellites. With the factor η increasing, the magnitude of splitting between $\rho_\uparrow$ and $\rho_\downarrow$ is enhanced, and the spin-up sub-peak becomes higher and higher but the spin-down one becomes smaller and smaller, which implies that spin-up electrons occupy the QD with a larger probability than the spin-down electrons do. In comparison with the case for the P alignment,[25] the shifted value of the Kondo peaks and Kondo satellites in the AP alignment is obviously small. It is emphasized that the asymmetry in the tunneling rates is essential to give rise to spin splitting for the AP magnetic configuration but not for the P one.

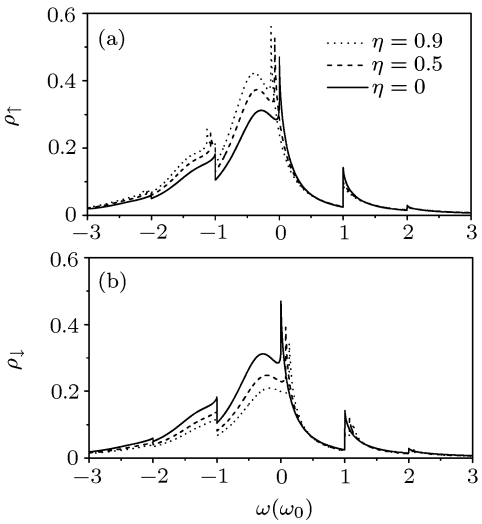


Fig.1. Spin-resolved DOSs, (a) $\rho_\uparrow$ and (b) $\rho_\downarrow$, as functions of energy ω for the indicated asymmetric factor η. The other parameters used are $\lambda = 0.5$, $B = 0$, and $V_{\rm bias} = 0$ and the magnetic moment is the AP alignment.

In what follows, we will discuss the nonequilibrium Kondo effect when the system considered is subjected to an applied bias voltage. First of all, we begin with the differential conductance, $G = G_\uparrow + G_\downarrow$, with spin-resolved differential conductances defined as $G_{\uparrow(\downarrow)} = \partial I_{\uparrow(\downarrow)}/\partial V_{\rm bias}$. Since the phonon-assisted Kondo satellites in the differential conductance appear at a large bias voltage and are not significant,[26] we focus on the main Kondo peak at a small bias voltage, where although phonon-assisted channels may be not open, the coupling of vibrational modes to electrons still modifies the transport properties to a certain extent.

As exhibited in Fig.2, it is evident that there is a significant difference in the differential conductances G between the P and AP configurations. At the symmetric case with $\eta = 0$ (solid lines), the Kondo peak for the P alignment splits into two sub-peaks, symmetrically located at the negative and positive bias

voltages, while there is no spin splitting and only a single peak is centered at the zero bias for the AP configuration. The splitting of the conductance peak for the P alignment has been observed in previous[11] and recent[12,13] experiments. Here, we further consider a more realistic situation when the tunneling barriers of the left-dot and right-dot contacts are different. With increasing asymmetric factor $\eta = 0,\ 0.3,\ 0.6,\ 0.9$ in turn from top to bottom, the Kondo peak for the AP alignment gradually becomes split, which is the reflection of the splitting in DOS. It is interesting to note that the splitting span for the AP case enlarges with enhancing η but it is independent of η for the P case. This can be understood from Eq.(7), from which it follows that the spin splitting $2g u_{\rm B} B_{\rm eff}^{(0)}$ is approximately proportional to $\Gamma_{\rm L0}+\Gamma_{\rm R0} = \Gamma_0$ for the P configuration and $\Gamma_{\rm L0} - \Gamma_{\rm R0} = \eta\Gamma_0$ for the AP case. In addition, as η increases, the differential conductances entirely decrease and eventually vanish at large η, independent of the magnetization configurations. On the other hand, one can notice that in the asymmetric case $\eta \neq 0$, the Kondo sub-peaks for both the P and AP alignments are asymmetric with bias voltage reversal and exhibit tilted profiles on the whole. However, the tilted directions of the conductance sub-peaks are different: the right sub-peak is higher than the left one for the P alignment but the left sub-peak is higher than the right one for the AP case. In order to clearly see the origin, the spin-resolved differential conductances G_σ with $\eta = 0.3$ are plotted in the corresponding insets. When the applied bias voltage is reversed from positive to negative, $G_\uparrow$ reduces and $G_\downarrow$ enhances for both the magnetic configurations. The competition between them gives the variation of total conductance G with bias voltage. For the P magnetic alignment, reducing of $G_\uparrow$ dominates and so the sub-peak in the positive bias is higher than the one in the negative bias. In contrast, the sub-peak in the negative bias is higher than the one in the positive bias for the AP alignment because enhancing of $G_\downarrow$ dominates in this magnetic situation.

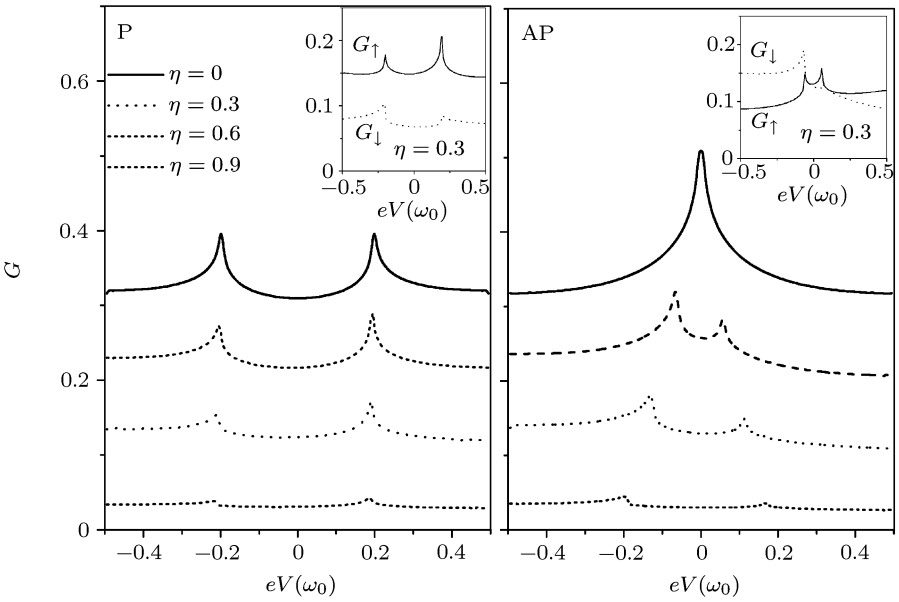


Fig.2. Differential conductances G as functions of bias voltage $V_{\rm bias}$ with $\eta = 0,\ 0.3,\ 0.6,\ 0.9$ for both the P and AP alignments. Spin-resolved differential conductances $G_{\uparrow(\downarrow)}$ with $\eta = 0.3$ for the P and AP configurations are, respectively, shown in the corresponding insets. The other parameters are the same as those in Fig.1.

The different behaviors of conductance sub-peaks in the P and AP will give rise to interesting tunneling magnetoresistance (TMR). The TMR ratio is defined as TMR$= (G_{\rm P} - G_{\rm AP})/G_{\rm AP}$, where $G_{\rm P}$ and $G_{\rm AP}$, respectively, stand for the differential conductances for the P and AP alignments. The phenomena of large negative TMR in the Kondo regime have been observed by recent experiment.[1] In Fig.3, we plot the

η-dependent TMR ratio vs. bias voltage, calculated from the differential conductances in Fig.2. When the experimental setup is asymmetric, one can notice that with increasing $\eta = 0$, 0.3, 0.6, 0.9 in turn, the zero-bias TMR exhibits a change from a single dip to two dips located at the positive and negative bias voltages, respectively. Furthermore, at large η the negative-bias TMR reduces rapidly and its sign changes, while the positive-bias TMR is dramatically enhanced, and is accompanied by a very high TMR peak. This asymmetry in the TMR ratio with respect to the bias reversal is due to opposite tilt directions in the differential conductances for the P and AP alignments.

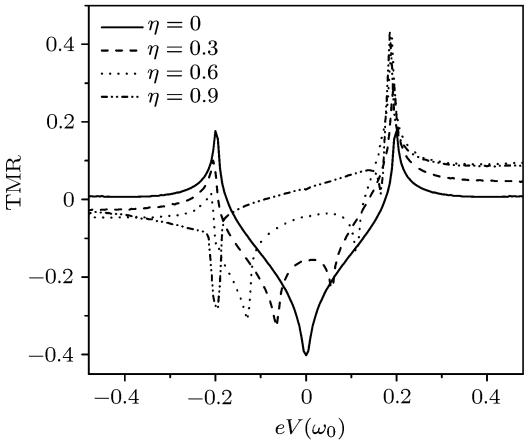


Fig.3. TMR ratios as functions of $V_{\rm bias}$ for $\eta = 0, 0.3, 0.6, 0.9$. The other parameters are the same as those in Fig.1.

From the above discussions, we know that the magnetism of the ferromagnetic electrodes to a certain extent suppresses and splits the zero-bias Kondo resonance due to the induced effective exchange field. If an inverse Zeeman energy is provided in the QD by applying an external magnetic field B, the effective exchange field will be completely compensated and the strong zero-bias Kondo resonance will be restored. Restoration of the Kondo peak has been successfully realized in experiments with carbon nanotubes[13] and semiconductor quantum dots[12] coupled to ferromagnetic electrodes. In order to understand the physics, in the following we shall study the case of the non-degenerated energy level, i.e. $\tilde{\varepsilon}_\sigma - \tilde{\varepsilon}_{\bar{\sigma}} = 2gu_{\rm B}B$. As some results resemble those in the absence of EPI addressed by Utsumi *et al*,[33] here we particularly focus on EPI-mediated restoration of the Kondo resonance in the presence of an applied magnetic field.

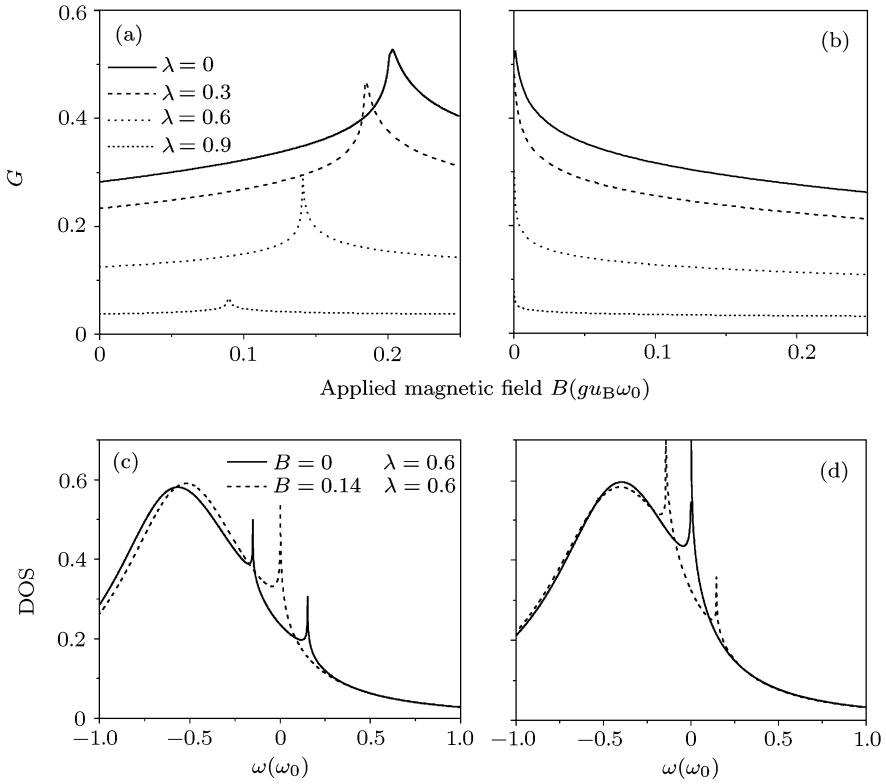


Fig.4. Zero-bias differential conductances G as functions of applied magnetic field B with EPI strength $\lambda = 0, 0.3, 0.6, 0.9$ for (a) P and (b) AP alignments. The DOSs in (c) and (d) correspond to the curves of $\lambda = 0.6$ in (a) and (b), respectively. $B = 0.14$ is the magnetic field to restore the Kondo peak for $\lambda = 0.6$.

Figure 4 exhibits the differential conductances (a) $G_{\rm P}$ and (b) $G_{\rm AP}$ at zero bias as functions of applied magnetic field B for different EPI strengths λ. From Fig.4(a) it can be seen that conductance $G_{\rm P}$ without magnetic field B is small due to the splitting of the Kondo peak. With increasing B, $G_{\rm P}$ increases and shows a remarkable peak at a certain field (referred to as a restoring field, e.g., $B = 0.14$ for $\lambda = 0.6$), which is evidence of restoration of the Kondo resonance. In this case, the applied external field B completely compensates the effective exchange field and smears out the splitting of the Kondo peak, as can be clearly seen from the dashed line in Fig.4(c), where double sub-peaks in the DOS are combined into a single peak when the restored magnetic field is $B = 0.14$. When the applied field B goes beyond the restoring field, the conductance $G_{\rm P}$ in Fig.4(a) reduces again due to the re-splitting of the restored Kondo peak in an excess magnetic field $B - B_{\rm eff}^{(0)}$. A different behavior is presented in Fig.4(b), where the conductance $G_{\rm AP}$ reaches its maximum at zero B and decreases with the field B in a monotonic way. This is because the Kondo peak in the DOS becomes split when it is subjected to the external field B, as shown in Fig.4(d). On the other hand, from Fig.4(a) one can note that EPI strength λ has a significant influence on the restoring field. When λ increases, the peak of differential conductance $G_{\rm P}$ shifts to the low magnetic field B, which results from the shrinking of the effective exchange field with increasing λ. In addition, both values of $G_{\rm P}$ and $G_{\rm AP}$ reduce fast in strong EPI.

A great difference between the variations of $G_{\rm P}$ and $G_{\rm AP}$ with EPI strength λ is shown to lead to an interesting behavior in the TMR ratio. In Fig.5, we plot the EPI-dependence of the zero-biased TMR ratios vs. applied field B. When the EPI strength λ increases, the peak of the TMR ratio gradually transfers from large to small field B owing to the reduction of the effective exchange field $B_{\rm eff}^{0}$. The whole behavior in the TMR ratio is dominated mainly by the behavior of the conductance $G_{\rm P}$ in Fig.4(a). In the meantime, there exhibits a non-monotonic behavior in the height of the TMR peak with λ changing, the highest TMR peak appearing at an intermediate EPI strength (i.e., $\lambda = 0.6$ for the chosen parameters). It is noted that the TMR ratio is very sensitive to the applied magnetic field, and so a fast switch from the negative TMR dip (about -50%) to the positive TMR peak (about -130%) can be manipulated by slightly modulating the external magnetic field, the magnitude of which greatly depends on the EPI coupling strength λ.

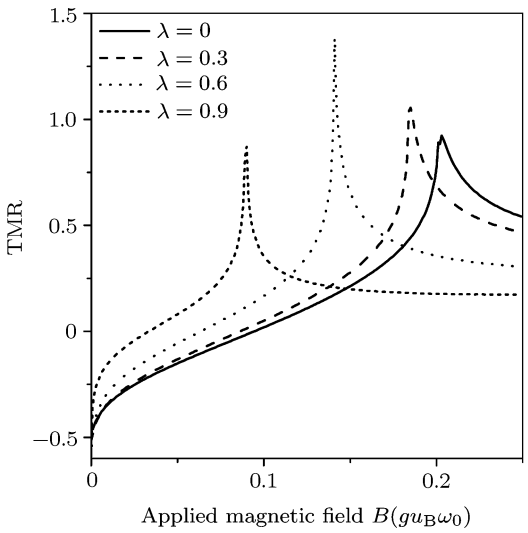


Fig.5. Zero-bias TMR ratios for different EPI strengths $\lambda = 0, 0.3, 0.6, 0.9$ as functions of applied magnetic field B.

4. Summary

In this paper, we have analyzed the nonequilibrium Kondo effect in spin-polarized electron transports through a single molecular QD coupled asymmetrically to ferromagnetic electrodes, with the molecular deformation described as interactions of the QD coupled to a phonon bath. The asymmetric coupling of QD to two ferromagnetic electrodes is essential to give rise to Kondo resonance splitting for the AP configuration but not for the P one. Since the effective exchange fields from two magnetic electrodes cannot completely compensate each other in the asymmetric AP configuration, both Kondo peaks of the Kondo resonance and the phonon-assisted Kondo satellites show spin splitting. The phonon-assisted Kondo satellites mostly mediate the DOS shape by the phonon energy. It is interesting to find that the asymmetric coupling tilts the profile of the spin-polarized Kondo sub-peaks in differential conductance, and the tilted directions are different for the two configurations. As a consequence, the curves of the double-dip TMR present a significant asymmetry with respect to the bias voltage in high asymmetry. On the other hand, we consider the compensation of the effective exchange field induced by the magnetism of leads. It is shown that restoration of the zero-bias Kondo resonance can be realized by an applied magnetic field B. A fast switch from the negative TMR dip to the positive TMR peak can be manipulated only by slightly modulating the external magnetic field, whose magnitude greatly depends on the EPI coupling strength.

References

[1] Yu L H, Keane Z K, Ciszek J W, Cheng L, Stewart M P, Tour J M and Natelson D 2004 *Phys. Rev. Lett.* **93** 266802

[2] Chen X W, He Z, Sun W L, Wu S Q and Yan C H 2006 *Acta Phys. Sin.* **55** 1413 (in Chinese)

[3] Martinek J, Utsumi Y, Imamura H, Barnaś J, Maekawa S, König J and Schön G 2003 *Phys. Rev. Lett.* **91** 127203

[4] Hou T, Wu S Q, Bi A H, Yang F B, Chen J F and Fan M 2009 *Chin. Phys.* B **18** 783

[5] Tang N Y 2009 *Acta Phys. Sin.* **58** 3397 (in Chinese)

[6] Zhang P, Xue Q K, Wang Y P and Xie X C 2002 *Phys. Rev. Lett.* **89** 286803

[7] Dong B, Cui H L, Liu S Y and Lei X L 2003 *J. Phys.: Condens. Matter* **15** 8435

[8] Choi M S, Sánchez D and López R, 2004 *Phys. Rev. Lett.* **92** 056601

[9] López R and Sánchez D 2003 *Phys. Rev. Lett.* **90** 116602

[10] Sergueev N, Sun Q F,Guo H,Wang B G and Wang J 2002 *Phys. Rev.* B **65** 165303

[11] Pasupathy A N, Bialczak R C, Martinek J, Grose J E, Donev L A K, Mceuen P L and Ralph D C 2004 *Science* **86** 306

[12] Hamaya K, Kitabatake M, Shibata K, Jung M, Kawamura M, Hirakawa K, Machida T, Taniyama T, Ishida S and Arakawa Y 2007 *Appl. Phys. Lett.* **91** 232105

[13] Hauptmann J R, Paaske J and Lindelof P E 2008 *Nature Physics* **4** 373

[14] Martinek J, Sindel M, Borda L, Barnaś J, Bulla R, König J, Schön G, Maekawa S and Delft J von 2005 *Phys. Rev.* B **72** 121302(R)

[15] Świrkowicz R, Wilczyński M and Barnaś J 2006 *J. Phys: Condens. Matter* **18** 2291

[16] Rochal A R, Suárez V M G, Bailey S W, Lambert C J, Ferrer J and Sanvito S 2005 *Naure Materials* **4** 335

[17] Pierre S, Anne B M and Frédéric P 2007 *J. Phys.: Condens. Matter* **19** 165222

[18] Yu L H, Keane Z K, Ciszek J W,Cheng L, Tour J M, Baruah T, Pederson M R and Natelson D 2005 *Phys. Rev. Lett.* **95** 256803

[19] Zhao A, Li Q X, Chen L, Xiang H J,Wang W H, Pan S, Wang B, Xiao X D, Yang J L, Hou J G and Zhu Q S 2005 *Science* **309** 1542

[20] Park H, Park J, Lim A K L Anderson E H, Alivisatos A P and McEuen P L 2000 *Nature* **407** 57

[21] Cao X S and Chen C L 2009 *Chin. Phys.* B **18** 2928

[22] Wu Z J, Yuan X Z, Zheng H and Zhu K D 2005 *Acta Phys. Sin.* **54** 3346 (in Chinese)

[23] Rudziński W 2008 *J. Phys.: Condens. Matter* **20** 275214

[24] Wang R Q, Zhou Y Q, Wang B G and Xing D Y 2007 *Phys. Rev.* B **75** 045318

[25] Wang R Q, Zhou Y Q and Xing D Y 2008 *J. Phys.: Condens. Matter* **20** 045219

[26] Świrkowicz R, Wilczyński M and Barnaś J 2008 *J. Phys.: Condens. Matter* **20** 255219

[27] Wang R Q, Wang B G and Xing D Y 2008 *Phys. Rev. Lett.* **100** 117206

[28] Meir Y and Wingreen N S 1992 *Phys. Rev. Lett.* **68** 2512

[29] Chen Z Z, Lu R and Zhu B F 2005 *Phys. Rev.* B **71** 165324

[30] Chen Z Z, Lu H Z, Lü R and Zhu B F 2006 *J. Phys: Condens. Matter* **18** 5435

[31] Meir Y, Wingreen N S and Lee P A 1991 *Phys. Rev. Lett.* **66** 3048

[32] Wilezyński M, Świrkowicz R and Barnaś J 2006 *Phys. Stat. Sol.(c)* **3** 105

[33] Utsumi Y, Martinek J, Schön G, Imamura H and Maekawa S 2005 *Phys. Rev.* B **71** 245116